The Journal of Immunology

A CD153^{+}CD4^{+} T Follicular Cell Population with Cell-Senescence Features Plays a Crucial Role in Lupus Pathogenesis via Osteopontin Production

Suhail Tahir, Yuji Fukushima, Keiko Sakamoto, Kyosuke Sato, Harumi Fujita, Joe Inoue, Toshimitsu Uede, Yoko Hamazaki, Masakazu Hattori and Nagahiro Minato

J Immunol 2015; 194:5725-5735; Prepublished online 13 May 2015;
doi: 10.4049/jimmunol.1500319
http://www.jimmunol.org/content/194/12/5725

The Journal of Immunology is published twice each month by
The American Association of Immunologists, Inc.,
9650 Rockville Pike, Bethesda, MD 20814-3994.

Print ISSN: 0022-1767 Online ISSN: 1550-6606.

A CD153$^+$CD4$^+$ T Follicular Cell Population with Cell-Senescence Features Plays a Crucial Role in Lupus Pathogenesis via Osteopontin Production

Suhail Tahir,* Yuji Fukushima,† Keiko Sakamoto,* Kyosuke Sato,* Harumi Fujita,* Joe Inoue,* Toshimitsu Uede,‡ Yoko Hamazaki,* Masakazu Hattori,† and Nagahiro Minato*

Immune aging results in diminished adaptive immunity and increased risk for autoimmunity. We previously reported a unique PD-1$^+$ CD44^{high}CD4$^+$ T cell population that increases with age in normal mice. In this study, we indicate that the age-dependent PD-1$^+$ CD44^{high}CD4$^+$ T cells develop as unique T follicular (TF) cells in a B cell–dependent manner and consist of two subpopulations, as follows: CD153$^+$ cells preferentially secreting abundant osteopontin on TCR stimulation and CD153$^-$ cells that are apparently TCR anergic. These unique TF cells with essentially similar features increase much earlier and are accumulated in the spontaneous germinal centers (GCs) in lupus-prone female BWF1 (f-BWF1) mice. These TF cells showed characteristic cell-senescence features and developed in association with extensive CD4$^+$ T cell proliferation in vivo, suggesting replicative senescence. Although the CD153$^+$ TF cells were defective in proliferation capacity, they were quite stable and specifically responded to self GC-B cells to secret abundant osteopontin, which inhibited B cell receptor–induced GC-B cell apoptosis in f-BWF1 mice. Transfer of CD153$^+$ PD-1$^+$ CD4$^+$ T cells promoted the growth of spontaneous GCs, whereas administration of anti-osteopontin Ab suppressed GC enlargement and anti-nuclear Ab production and ameliorated clinical lupus nephritis of f-BWF1 mice. Current results suggest that senescent CD153$^+$ TF cells generated as a consequence of extensive endogenous CD4$^+$ T cell proliferation play an essential, if not sufficient, role in lupus pathogenesis in lupus-prone genetic background and may also contribute to an increased autoimmunity risk with age. ***The Journal of Immunology*****, 2015, 194: 5725–5735.**

Germinal centers (GCs) are unique niches in secondary lymphoid tissues in which a specific Ab response occurs after Ag immunization (1). In GCs, Ag-specific B cells undergo a series of dynamic processes, including robust proliferation, somatic hypermutation, and class-switch recombination of BCR genes, affinity maturation, and differentiation into memory or plasma cells (2). The initiation of GC reaction requires Ag-specific T cells (3). After Ag immunization, some of these T cells migrate into the follicular B cell region to regulate specific GC reactions and are called T follicular (TF) cells (4–6). Accumulating evidence indicates that functionally distinct types of T cells may be recruited to GCs, including TF helper (TFH) cells, regulatory T cells, and NKT cells (7).

GC reactions may occur spontaneously in various autoimmune diseases, including lupus (8, 9). Lupus disease, which preferentially affects young females in humans, is a multifactorial disease affecting various organs, most commonly glomerulonephritis. A hallmark of the disease is production of autoantibodies against a diverse spectrum of self-Ags, including nuclear components (10, 11). Among several immune disorders in lupus is a defective checkpoint of B cell self-tolerance (12). Although potentially self-reactive B cells are normally excluded from GCs, they are included in GCs in the lupus-prone genetic background, leading to overt autoantibody production (13, 14). Recent studies highlight an important role of TF cells in the spontaneous GC reactions of lupus disease (15–17). However, it remains elusive how such spontaneous GC reactions develop and are regulated.

We previously identified a PD-1$^+$ CD44^{high}CD62L^{low}CD4$^+$ T cell population that steadily increases age dependently in normal B6 mice (18). The CD4$^+$ T cell population, termed senescence-associated T (SA-T) cells, shows unique genetic signature and functional features, including attenuated TCR-mediated proliferation and highly biased secretion of osteopontin (OPN), suggesting their contribution to reduced acquired immunity and increased inflammatory trait in senescence (18). Most recently, it was reported that unique TF cells with a similar genetic signature to SA-T cells were increased in *B6.Sle1b* congenic mice (19), which develop anti-nuclear Abs (ANAs) but no clinical disease (11). Although Slamf6 receptor coded in a *Sle1b* gene cluster was indicated to play a crucial role in the increase of TF cells and ANA production (19), the origin and relation of them with SA-T cells remain unknown.

*Department of Immunology and Cell Biology, Graduate School of Medicine, Kyoto University, Kyoto 606-8501, Japan; †Center for Innovation in Immunoregulative Technology and Therapeutics, Graduate School of Medicine, Kyoto University, Kyoto 606-8501, Japan; and ‡Division of Molecular Immunology, Institute for Genetic Medicine, Hokkaido University, Sapporo 060-0815, Japan

Received for publication February 10, 2015. Accepted for publication April 17, 2015.

This work was supported by a Grant-in-Aid for Scientific Research on Innovative Areas from the Japan Society for the Promotion of Science; Special Coordination Funds for Promoting Science and Technology from the Japanese Government; the "Formation of Innovation Center for Fusion of Advanced Technologies" program of Astellas Pharma, Inc.; the Uehara Memorial Foundation; and Ono Pharmaceutical Co., Ltd.

Address correspondence and reprint requests to Prof. Nagahiro Minato, Department of Immunology and Cell Biology, Graduate School of Medicine, Kyoto University, Kyoto 606-8501, Japan. E-mail address: minato@imm.med.kyoto-u.ac.jp

The online version of this article contains supplemental material.

Abbreviations used in this article: ANA, anti-nuclear Ab; EGFP, enhanced GFP; f-BWF1, female BWF1; GC, germinal center; miR, microRNA; OPN, osteopontin; PNA, peanut agglutinin; SA-T, senescence-associated T; TF, T follicular; TFH, TF helper.

www.jimmunol.org/cgi/doi/10.4049/jimmunol.1500319

In the current study, we indicate that SA-T cells develop as a unique TF cell population in normal B6 mice with age and much prematurely in bone fide lupus-prone female BWF1 (f-BWF1) mice, in association with spontaneous GC reactions. The SA-T cells in both aged B6 mice and f-BWF1 mice are developed in association with extensive endogenous CD4$^+$ T cell proliferation in vivo and show characteristic cell-senescence features. We demonstrate that a minor cell population expressing CD153 in the SA-T cells plays a crucial role in spontaneous GC reactions and development of clinical lupus nephritis.

Materials and Methods

Mice

New Zealand White, New Zealand Black, New Zealand Black × New Zealand White F_1 (BWF1), and C57BL/6 (B6) mice were purchased from Japan SLC, and μMT mice were provided by M. Reth (Albert Ludwigs Universität Freiburg, Freiburg, Germany). The enhanced GFP (EGFP)-OPN reporter mice were generated as a custom order via Unitech (Kashiwa, Chiba, Japan). In brief, the *Spp1* chromosomal gene was isolated from bacterial artificial chromosome clones of C57BL/6 mice, and its exon 2 was replaced by a coding sequence for *EGFP* and *loxp*-neo-*loxp* genes. The targeting vector containing the diphtheria toxin A fragment upstream exon 1 was transfected into embryonic stem cells (clone: Bruce 4) derived from C57BL/6 mice (20). The embryonic stem clones carrying the *Spp1*-deficient allele were introduced into host embryos, and the chimeric mice were crossed with the CAG-Cre transgenic. All mice were maintained under specific pathogen-free conditions at the Centre for Experimental Animals of Kyoto University, and the animal experiments were performed in accordance with the institutional guidelines.

Cells and cultures

WEHI231 (mouse B1 cell) line was provided by K. Iwai (Kyoto University, Kyoto, Japan). Sorted CD4$^+$ T cell subpopulations were cultured in round-bottom 96-well plates (1×10^5 cells) in the presence of coated anti-CD3 (1 μg/well) and soluble anti-CD28 (2.5 μg/ml) Abs, or with autologous B cells (1×10^6 cells) preirradiated with 15 Gy γ-ray. Anti-MHC II (BioLegend), anti–PD-1 (RMP1-14), anti–PD-L1, anti–PD-L2, anti-CD40 Ab (HM40-3; eBioscience), PD-L1-Ig (R&D Systems), or CD30-Ig fusion protein (21) (provided by N. Yoshikai, Institute of Bioregulation, Kyushu University, Fukuoka, Japan) was additionally included in the culture. Recombinant OPN (R&D Systems) was used in an immobilized form. Cell viability was assessed by Cell Titer-Glo luminescent cell viability assay (Promega).

Cytokines and autoantibodies

OPN and other cytokines in the culture supernatants were assessed with ELISA kits. Autoantibodies were also measured with ELISA kits (Shibayagi).

Flow cytometry

Multicolor flow cytometric analysis and cell sorting were performed with FACS Canto and FACS Aria II/III (BD Biosciences), respectively. The following Abs were used: PE-conjugated anti-ICOS, anti-CD200, anti-CD153, anti-CD121b, anti–IL-21, anti-CD30, anti-OPN, anti–PD-L1, anti–PD-L2, and anti-peanut agglutinin (PNA; BioLegend); anti-CXCR5, Alexa647-conjugated anti–PD-1, FITC-conjugated anti-CD44, anti-GL7, anti-B220, and anti-annexin V, Cy7-conjugated anti-CD95 (BD Biosciences); and FITC-conjugated anti-Ki67 (eBioscience). For intracellular staining of cytokines, cells were incubated with PMA (20 ng/ml) and ionomycin (1 μg/ml) in the presence of brefeldin A for 5 h before the analysis.

Immunostaining

Tissues were snap frozen in optimum cutting temperature compound (Sakura). Serial frozen sections were fixed with 95% ethanol, followed by 100% acetone. Immunostained sections were mounted in Mowiol (Calbiochem) and examined under a microscope (Carl Zeiss). Abs included anti-B220, anti-CD4, anti-CD8, anti–PD-1 (BioLegend), anti-GL7 (eBioscience), and anti-CD3 (BD Biosciences). GC areas were assessed with the use of Axio Vision 4.8.2 SP1 software. Tile images of whole tissue sections were generated using the MosaiX tool of Zeiss Axiovision software (Carl Zeiss). For heterochromatin staining, cells were cytospun, fixed for 10 min in 4% paraformaldehyde, and permeabilized with 0.1% Triton X-100 PBS for 10 min. After blocking, the cells were incubated with anti–HP-1β Ab (Millipore), followed by fluorophore Alexa488-conjugated secondary Ab and DAPI.

Laser-capture microdissection

Cryostat sections were affixed to frame membrane slides for the Arcturus^{XT} LMD system (Life Technologies), fixed in acetone, and stained with biotinylated PNA and HistoGene immunofluorescence staining kit. After dehydration, the regions of interest were dissected on an Arcturus^{XT} system (Life Technologies).

Quantitative PCR

Quantitative PCR was performed with SYBR Green I Master mix (Roche) on a LightCycler 480 (Roche). Cyclophilin and U6 RNA were used as internal controls for mRNA and microRNAs (miRs), respectively. Primer sequences for genes and miR are as follows: *Tnfsf8*, 5′-GAGGATCTCTTCTGTACCCTGAAA-3′ and 5′-TTGGTATTGTTGAGATGCTTTGA-3′; *Spp1*, 5′-CCCGGTGAAAGTGACTGATT-3′ and 5′-TTCTTCAGAGGACACAGCATTC-3′; *Il1r2*, 5′-CCCATCCCTGTGATCATTTC-3′ and 5′-GCACGGGACTATCAGTCTTGA-3′; *Ccl3*, 5′-TCTGTCACCTGCTCAACATCA-3′ and 5′-CGGGGTGTCAGCTCCATA-3′; *Cebpa*, 5′-AAACAACGCAACGTGGAGA-3′ and 5′-GCGGTCATTGTCACTGGTC-3′; *Cdkn1a*, 5′-AACATCTCAGGGCCGAAA-3′ and 5′-TGCGCTTGGAGTGATAGAAA-3′; *Cdkn2b*, 5′-AATAACTTCCTACGCATTTTCTGC-3′ and 5′-CCCTTGGCTTCAAGGTGAG-3′; *Cd30*, 5′-GTCCACGGGAACACCATTT-3′ and 5′-CCAACCAGTAGCACCACCAT-3′; *Bcl2a1a*, 5′-TTTCCAGTTTTGTGGCAGAAT-3′ and 5′-TCAAACTTCTTTATGAAGCCATCTT-3′; and *miR-181a*, 5′-AGGTCAACATTCAACGCTGTC-3′ and 5′-CTCAACTGGTGTCGTGGAGTC-3′.

Cell transfer and Ab administration

Sorted T cell subpopulations were suspended in temperature-sensitive biogel (Mebiol Gel; Mebiol) at 4°C and directly injected into spleens of anesthetized mice. Mouse anti-OPN Ab (35B6) (22) or isotype-matched mouse IgG (Sigma-Aldrich) was administered i.p. at 500 μg per mouse twice per week.

Statistical analyses

Statistical analyses were performed by Student *t* test.

Results

SA-T cells are developed and accumulated spontaneously with age as unique TF cells

Normal mice show a progressive increase in a PD-1$^+$ CD44^{high}CD4$^+$ T cell population with age, termed SA-T cell population, which shows attenuated proliferative response, but secretes large amounts of OPN on TCR stimulation (18). Immunostaining analysis revealed that PD-1$^+$ CD4$^+$ T cells were mainly distributed in splenic follicular regions with a significant accumulation in PNA$^+$ GCs, which spontaneously developed in aged B6 mice (Fig. 1A). The PD-1$^+$ CD4$^+$ T cells significantly expressed CXCR5 similar to TFH cells induced by SRBC immunization (Fig. 1B). Because our previous DNA microarray analysis revealed a marked increase in *Cd153* expression in SA-T cells compared with the PD-1$^-$ counterpart cells (18), we examined the cell surface expression of CD153 on them. A minor portion of them expressed CD153, which was rarely expressed in SRBC-TFH cells (Fig. 1B). Both CD153$^+$ and CD153$^-$ fractions also showed a high expression of TF-related genes such as *Bcl6*, *Cebpa*, and *Cxcr5*, although the levels tended to be less than those in SRBC-TFH cells (Fig. 1C). Both fractions additionally showed a markedly increased expression of proinflammatory genes, such as *Spp1*, *Ccl3*, and *Il1r2*, which were barely expressed in SRBC-TFH cells (Fig. 1C). Regardless of the expression of CD153, the age-dependent development of SA-T cells was remarkably reduced in μMT mice and thus required B cells (Fig. 1D). However, the two subsets of SA-T cells revealed quite distinct TCR responsiveness. Thus, CD153$^+$ SA-T cells secreted large amounts of OPN with less proliferation than PD-1$^-$ CD4$^+$ T cells via optimal TCR stimulation in vitro, whereas CD153$^-$ SA-T cells showed no detectable proliferation or production of cytokines at all, including OPN, despite higher basal *Spp1* expression than PD-1$^-$ CD4$^+$ T cells (Fig. 1E). As expected, SRBC-TFH cells produced IL-4 and less amounts of IFN-γ and IL-2, but no OPN

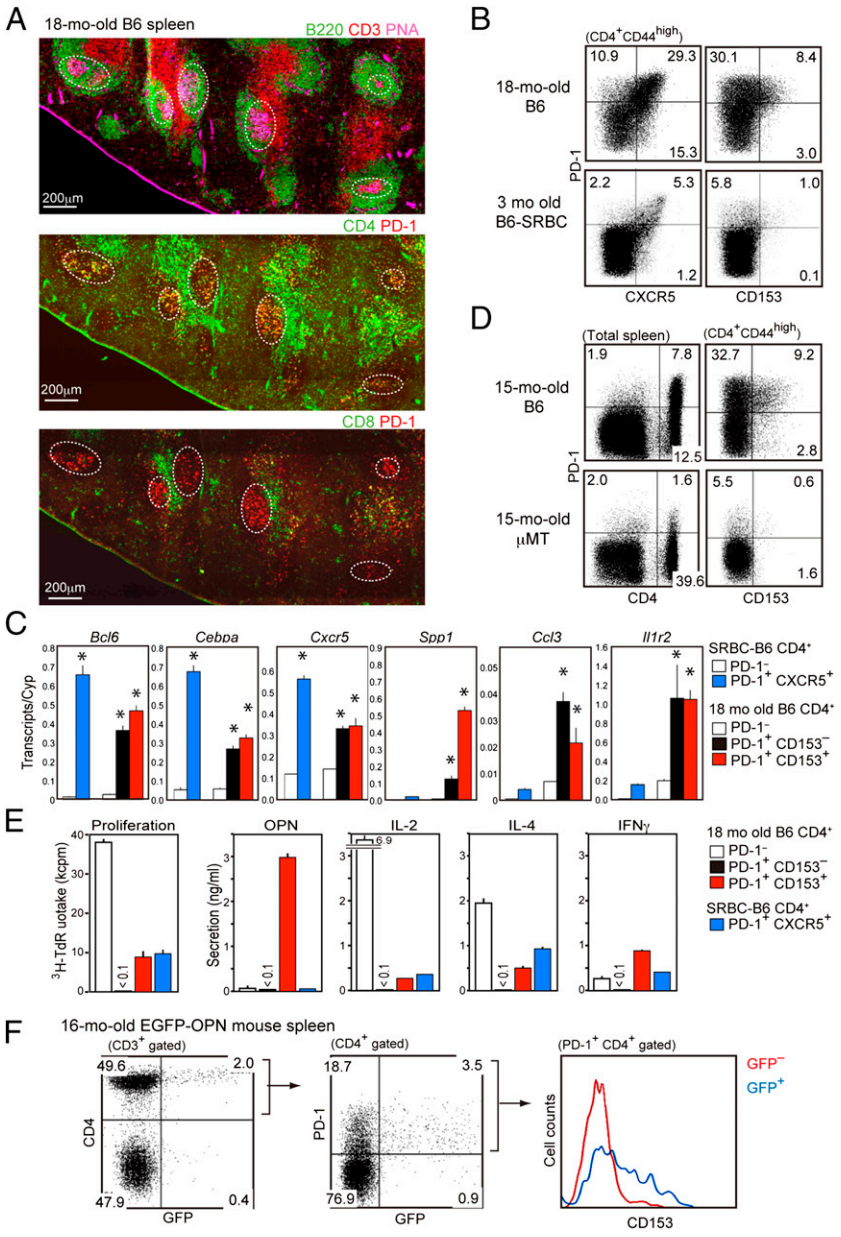

FIGURE 1. SA-T cells develop as unique TF cells with age in B6 mice. (**A**) Consecutive sections of the spleen from 18-mo-old B6 mice were multicolor immunostained with indicated Abs. Dotted circles indicate PNA^+ GCs. (**B**) Spleen cells from B6 mice at the age of 18 mo and those from 3-mo-old B6 mice that were immunized with SRBC 7 d before were multicolor analyzed with indicated Abs. (**C**) $PD\text{-}1^-$, $PD\text{-}1^+$ $CD153^-$, and $PD\text{-}1^+$ $CD153^+CD4^+$ T cells from aged B6 mice as well as $PD\text{-}1^+$ $CXCR5^+CD4^+$ T cells from SRBC-immunized B6 mice were sorted, and the expression of indicated genes was assessed with quantitative RT-PCR. The means and SEs of triplicate determination are shown. $*p < 0.01$. (**D**) Spleen cells from μMT and littermate control mice at the age of 18 mo were analyzed for the expression of indicated markers. (**E**) The cells isolated as in (C) were cultured in the presence of solid-phase anti-CD3 and soluble anti-CD28 Abs. Three days later, cell proliferation and cytokine production were assessed. The means and SEs of triplicate culture are shown. (**F**) Spleen cells from EGFP-OPN knock-in mice at the age of 16 mo were analyzed for the expression of indicated markers at the shown cell gates.

(Fig. 1E). We then validated the expression of OPN in $CD153^+$ SA-T cells in vivo with the use of EGFP-OPN knock-in mice. A significant portion of $PD\text{-}1^+$ $CD4^+$ cells selectively expressed quite high levels of GFP in 18-mo-old EGFP-OPN mice (Fig. 1F). Moreover, GFP^+ cell fraction of the $PD\text{-}1^+$ $CD4^+$ cells showed a higher expression of CD153 than corresponding GFP^- cell fraction, indicating that $CD153^+$ SA-T cells actually showed a potent *Spp1* activation spontaneously in vivo in aged mice (Fig. 1F). Although significant proportions of other cell types in the spleen also expressed GFP, including $B220^+$ B cells and $CD11b^+$ myeloid cells, the extents were by far less than that of $PD\text{-}1^+$ $CD4^+$ cells (Supplemental Fig. 1). The results suggest that SA-T cells develop as TF cells with unique functional features in a B cell–dependent manner.

Premature and systemic increase in TF cells highly resembling SA-T cells in bona fide lupus-prone f-BWF1 mice

Above findings prompted us to investigate the TF cells in f-BWF1 mice, which robustly develop spontaneous GCs preceding the overt clinical disease (Supplemental Fig. 2). F-BWF1 mice at as early as 6 mo of age showed a remarkable increase in $PD\text{-}1^+$ $CD44^{high}CD4^+$ T cells, and significant portions of them expressed CXCR5 and CD153, similar to SA-T cells; 2-mo-old f-BWF1 mice barely developed such a population (Fig. 2A). Furthermore, the expression of TF cell–related genes, *Bcl6*, *Cebpa*, and *Cxcr5*, as well as genes that were uniquely increased in SA-T cells, *Spp1*, *Ccl3*, and *Il1r2*, was also remarkably increased in both $CD153^+$ and $CD153^-$ fractions of the $PD\text{-}1^+$ $CD4^+$ T cells (Fig. 2B). Functionally, $CD153^+$ population secreted abundant OPN and Ccl3 with much lower levels of IL-2, IL-4, IL-5, and IFN-γ via TCR stimulation, whereas the $CD153^-$ cells produced little or no detectable cytokines at all (Fig. 2C). We failed to detect the secretion of IL-21, which plays an important role in Ag-driven GC reactions (23), in either $CD153^+$ or $CD153^-$ TF cell fraction with ELISA. However, intracellular staining indicated a significant IL-21 expression in both fractions, whereas OPN expression was mostly confined to the $CD153^+$ fraction (Supplemental Fig. 3). Furthermore, the majority of OPN^+ TF cells did not coexpress IL-21 in aged EGFP-OPN mice (Supplemental Fig. 3). Interestingly, $PD\text{-}1^+$ $CD4^+$ T cells were significantly more stable in culture than $PD\text{-}1^-$

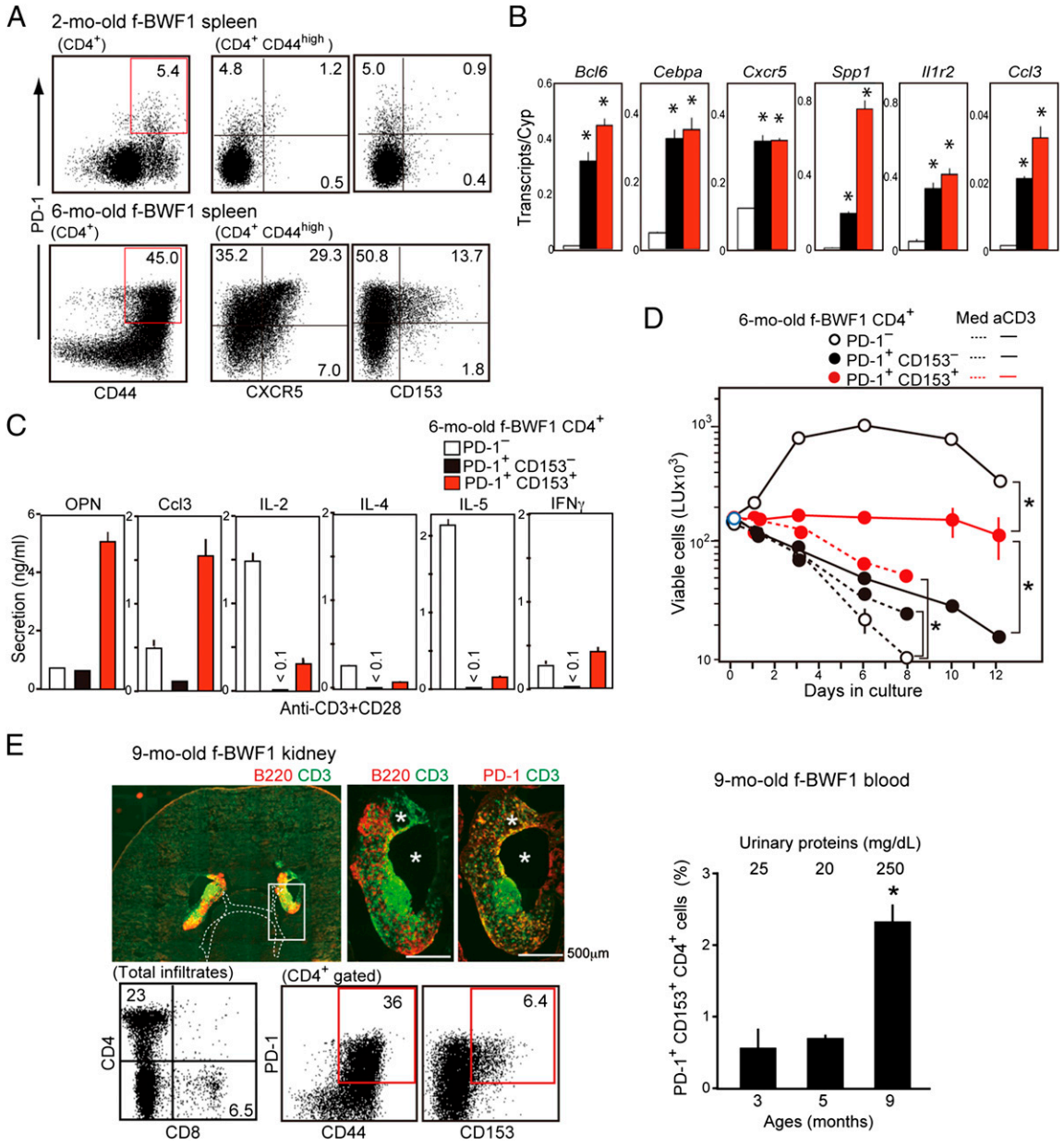

FIGURE 2. TF cells in f-BWF1 mice highly resemble the SA-T cells in aged B6 mice. (**A**) Spleen cells from f-BWF1 mice at the age of 2 and 6 mo were multicolor analyzed with indicated Abs. (**B**–**D**) PD-1$^-$, PD-1$^+$ CD153$^-$, and PD-1$^+$ CD153$^+$CD4$^+$ T cells were sorted from 6-mo-old f-BWF1 mice, and the expression of indicated genes was assessed with quantitative RT-PCR (B). The means and SEs of triplicate determination are shown. Aliquots of these cells were cultured in the presence of solid-phase anti-CD3 and soluble anti-CD28 Abs. Three days later, cell proliferation and cytokine production were assessed (C). Varying days after the culture, viability of these cells was also assessed by Cell Titer-Glo luminescent assay (D). The means and SEs of triplicate culture are shown. (**E**) Kidneys from 9-mo-old f-BWF1 mice were immunostained with indicated Abs, and the infiltrated cells in the kidneys were analyzed for the expression of indicated markers (*left*). The percentages of PD-1$^+$ and CD153$^+$ cells in a CD4$^+$ T cell gate are indicated. The peripheral blood of these mice was also analyzed, and the proportions of PD-1$^+$ CD153$^+$ cells in CD4$^+$ T cell fraction were assessed, along with urinary protein levels (*right*). The means and SEs of three mice are shown. $*p < 0.01$.

CD4$^+$ T cells (Fig. 2D). The stability of CD153$^+$ cells was further enhanced with no actual cell increase in the presence of coated anti-CD3 Ab; the viability of CD153$^-$ cells was barely affected, whereas PD-1$^-$ CD4$^+$ T cells were remarkably increased, as expected (Fig. 2D). The results suggested that the apparent TCR unresponsiveness of CD153$^-$ cells was unlikely due to activation-induced cell death. At later stages, when clinical nephritis became evident, PD-1$^+$ CD4$^+$ T cells, including CD153$^+$ cells, were significantly detected in the circulation as well as in the tertiary lymphoid structures of the affected kidneys (Fig. 2E). The results suggest that TF cells highly resembling SA-T cells are increased in f-BWF1 mice much earlier than in B6 mice and may recirculate to lupus target organs as the disease advances.

Lupus TF cells and SA-T cells show cell-senescence features in common and increase in association with extensive CD4$^+$ T cell proliferation in vivo

Given the similarity of TF cells in f-BWF1 mice and SA-T cells, we sought for basic cellular features underlying the two cell populations. CD153$^+$, and to a lesser extent CD153$^-$, PD-1$^+$ CD4$^+$ T cells in both f-BWF1 mice and aged B6 mice revealed a remarkably increased expression of *Cdkn2b* (*Ink4b*) and *Cdkn1a* (*Cip1*), which are typical cell-senescence biomarker genes (24), compared with corresponding

PD-1$^-$ CD4$^+$ T cells; this was not the case for SRBC-TFH cells (Fig. 3A, *left*). It is reported that the expression of miR-181a decreases age dependently in human CD4$^+$ T cells (25). The expression of miR-181a was decreased with age also in mouse PD-1$^-$ CD4$^+$ T cells; however, PD-1$^+$ CD4$^+$ T cells, in particular CD153$^+$ population, showed much more profound decrease than PD-1$^-$ cells in both aged B6 mice and f-BWF1 mice, and accordingly, an increased expression of target tyrosine phosphatase genes such as *Ptpn11* (Fig. 3A, *right*). Furthermore, PD-1$^+$ CD4$^+$ T cells in both groups of mice revealed a remarkable increase in senescence-associated heterochromatic foci in

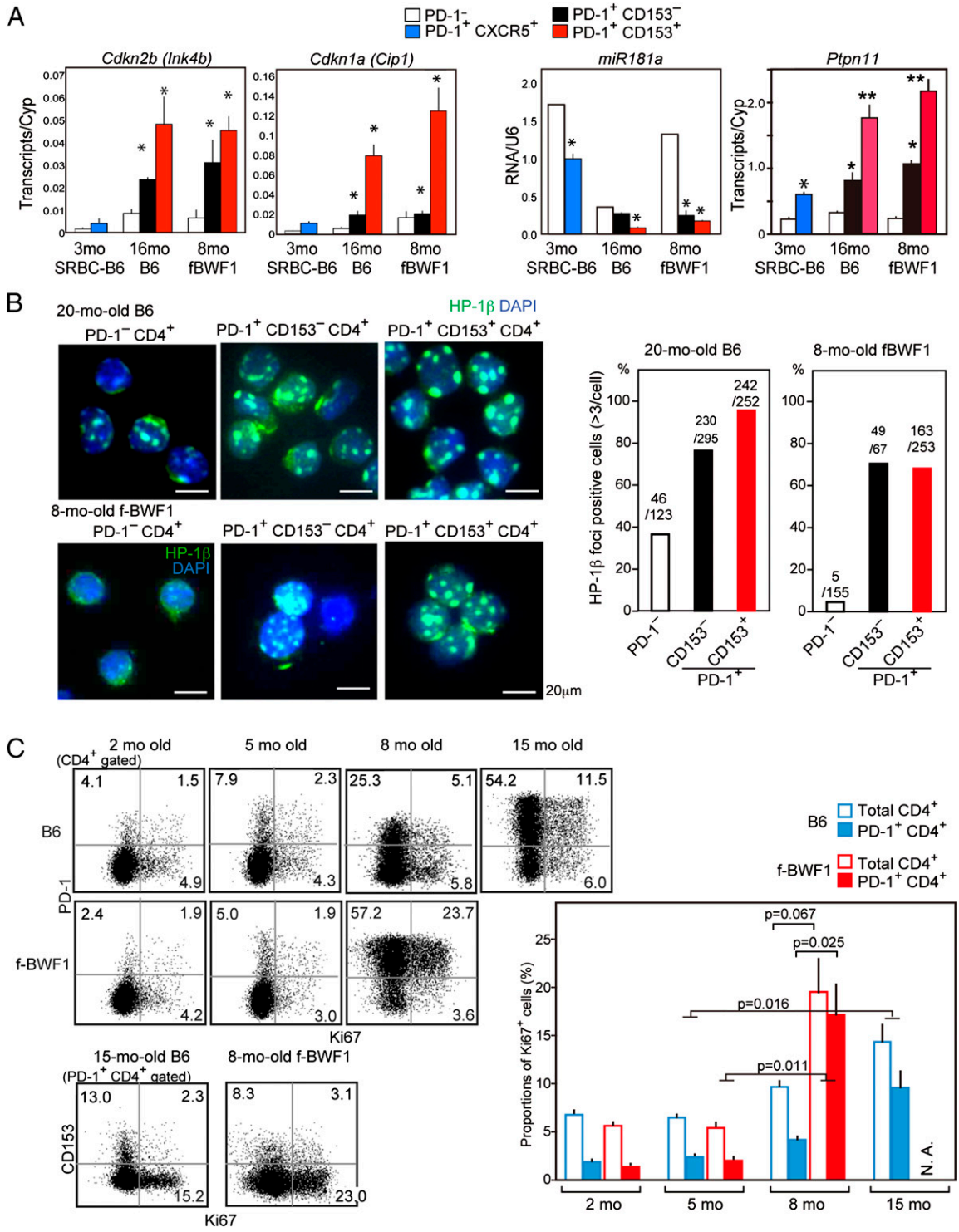

FIGURE 3. Lupus TF cells and SA-T cells increase correlating with extensive CD4$^+$ T cell proliferation in vivo and show cell-senescence features. (**A** and **B**) PD-1$^-$, PD-1$^+$ CD153$^-$, and PD-1$^+$ CD153$^+$CD4$^+$ T cells were sorted from the spleens of 16-mo-old B6 mice and 6-mo-old f-BWF1 mice and analyzed for the expression of indicated genes and miR, in comparison with PD-1$^-$ and PD-1$^+$ CXCR5$^+$CD4$^+$ T cells from 3-mo-old B6 mice that were immunized with SRBC 7 d before (A). The means and SEs of riplicate determination are shown. Aliquots of these cells were cytospun and immunostained with anti–HP-1β and DAPI (B). The numbers of cells showing more than three HP-1β$^+$ foci/total counted cells are indicated. (**C**) Spleen cells from B6 and f-BWF1 mice matched at various ages were analyzed for the expression of indicated markers (*left*). The proportions of Ki67$^+$ cells in the indicated cell populations are indicated (*right*). The means and SEs of four mice at each age are shown. F-BWF1 mice did not survive until the age of 15 mo (N.A.). *$p < 0.01$,**$p < 0.001$.

the nuclei (26) (Fig. 3B). Thus, TF cells in both mice show cell-senescence features in common. One of the main causes for cell senescence is extensive cell proliferation, and therefore we examined the proliferative state of $CD4^+$ T cells in vivo. Adult B6 mice at the ages younger than 8 mo had low levels of $Ki67^+$ cycling $CD4^+$ T cells that minimally expressed PD-1; however, 15-mo-old B6 mice showed a significant increase in the $Ki67^+$ $CD4^+$ T cells, and the majority of them expressed PD-1 (Fig. 3C). F-BWF1 mice revealed a remarkable increase in $Ki67^+$ $CD4^+$ T cells as early as 8 mo of age, and again most of these cells showed PD-1 expression (Fig. 3C). Notably, however, $CD153^+$ cells in the $PD\text{-}1^+$ $CD4^+$ T cell populations of both mice contained only minimal $Ki67^+$ cells (Fig. 3C). The findings are in agreement with much higher expression of cdk inhibitors, *Ink4b* and *Cip1*, in $CD153^+$ cells than in $CD153^-$ cells. These results suggest that the increase of $PD\text{-}1^+$ $CD4^+$ TF cells is attributable to extensive $CD4^+$ T cell proliferation in vivo, which occurs much earlier and more robustly in f-BWF1 than in B6 mice, eventually resulting in the accumulation of cell-senescent $CD153^+$ cell population.

Senescent $CD153^+$ $PD\text{-}1^+$ $CD4^+$ TF cells in f-BWF1 mice produce OPN in response to autologous GC B cells via PD-1–resistant, CD153-costimulated TCR signal

Inasmuch as the development of SA-T cells was B cell dependent, we next investigated the functional interaction of them with B cells in f-BWF1 mice. The $CD153^+$ $PD\text{-}1^+$ $CD4^+$ T cells from f-BWF1 mice secreted significant amounts of OPN in the coculture with γ-ray–irradiated autologous B cells, whereas $PD\text{-}1^-$ and $CD153^-$ $PD\text{-}1^+$ $CD4^+$ T cells did not and did so only minimally, respectively; among the B cells, the stimulatory activity of $CD95^+$ ($GL7^+$ or $GL7^-$) GC B cells was more potent than that of $CD95^-$ B cells (Fig. 4A). The OPN production by $CD153^+$ cells in response to B cells was inhibited significantly in the presence of anti-MHC II Ab cross-reactive with both $I\text{-}A^d$ and $I\text{-}A^u$ and almost completely by soluble anti-CD3 Ab (Fig. 4A), confirming the TCR-mediated activation. However, although GC B cells significantly expressed PD-L1 and PD-L2, the GC B cell–induced OPN production was not affected by anti–PD-L1 or anti–PD-L2 Ab at all (Fig. 4B). Furthermore, OPN production by $CD153^+$ cells in the presence of

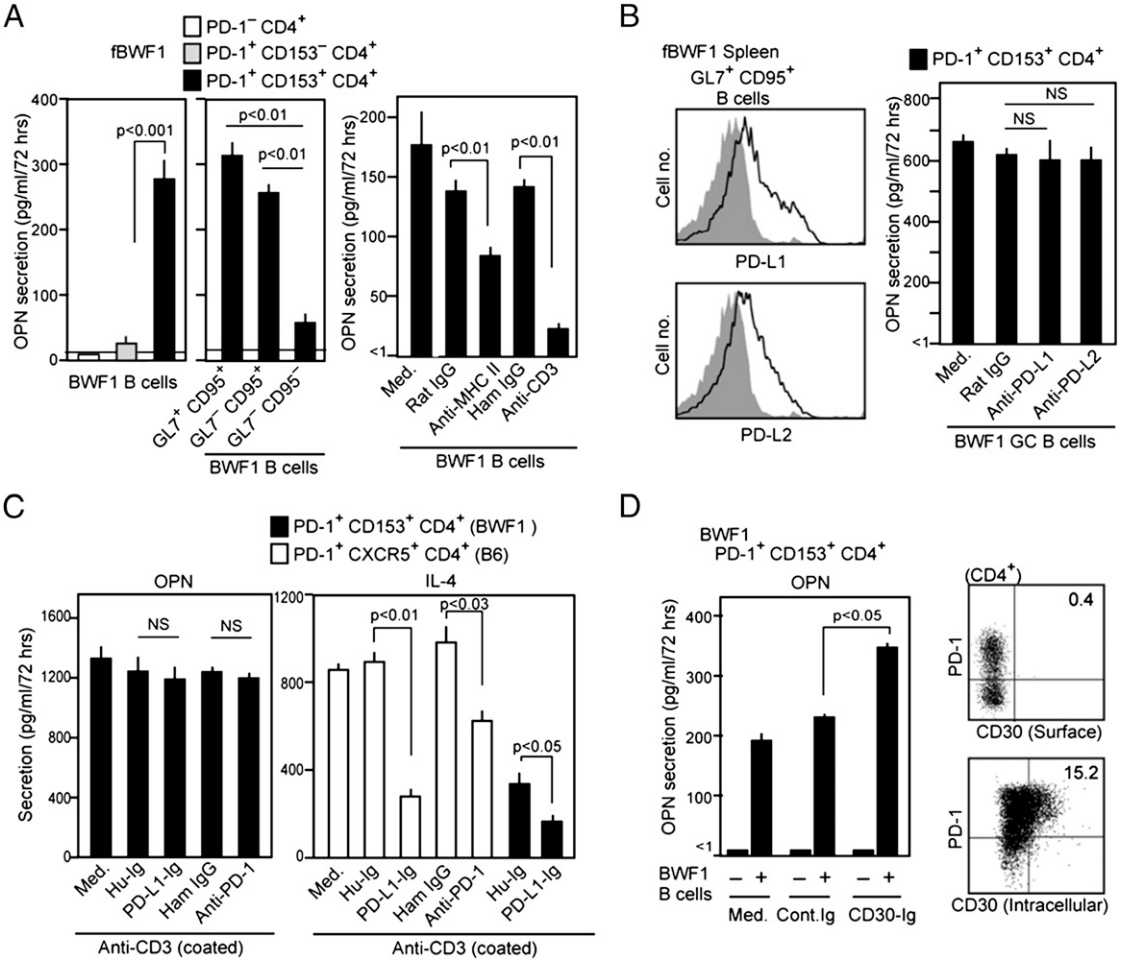

FIGURE 4. $CD153^+$ SA-T cells from f-BWF1 mice produce OPN in response to autologous GC B cells via PD-1–resistant TCR signaling. (**A**) Splenic $PD\text{-}1^-$, $PD\text{-}1^+$ $CD153^-$, and $PD\text{-}1^+$ $CD153^+CD4^+$ T cells isolated from female BWF1 mice were cultured with γ-ray–irradiated total or indicated subpopulations of B cells in the absence or presence of soluble anti–MHC-II, anti-CD3, or control IgG (50 μg/ml each). Three days later, OPN in the culture supernatants was assessed. The means and SEs of triplicate culture are indicated. (**B**) $CD153^+$ SA-T cells from female BWF1 mice were cultured with GC B cells in the presence of anti–PD-L1, anti–PD-L2, or control IgG (50 μg/ml each). Surface expression of PD ligands on the GC B cells is also shown. (**C**) $PD\text{-}1^+$ $CD153^+CD4^+$ and $PD\text{-}1^+$ $CXCR5^+CD4^+$ T cells were sorted from female BWF1 mice and SRBC-immunized B6 mice, respectively, and cultured in the presence of coated anti-CD3 Ab along with PD-L1-Ig, anti–PD-1 Ab, or control reagents. Three days later, the secretion of OPN and IL-4 was assessed. Means and SEs of triplicate culture are indicated. (**D**) The sorted $PD\text{-}1^+$ $CD153^+CD4^+$ T cells from f-BWF1 mice were cultured with irradiated autologous B cells in the absence or presence of control Ig or CD30-Ig (20 μg/ml), and, 3 d later, the secretion of OPN was assessed (*left*). Means and SEs of triplicate culture are indicated. Aliquots of the cultured cells on day 3 were analyzed for cell surface (*top right*) and intracellular (*bottom right*) CD30 expression.

coated anti-CD3 Ab was not affected by either solid-phase PD-L-Ig or anti–PD-1 Ab, whereas a low level of IL-4 production was significantly inhibited by PD-L-Ig, similarly to the IL-4 production by SRBC-TFH cells (Fig. 4C). In contrast, OPN production by $CD153^+$ cells in response to B cells was significantly enhanced in the presence of CD30-Ig (Fig. 4D). Although cell surface CD30 expression was barely detected in normal splenic cells, $PD\text{-}1^+$ $CD4^+$ TF cells showed significant intracellular expression of CD30 after the coculture with B cells (Fig. 4D), suggesting a possible involvement of shed CD30 in the reverse CD153 activation (27). The results suggest that senescent $CD153^+$ $PD\text{-}1^+$ $CD4^+$ TF cells in f-BWF1 mice are self-reactive and are activated to produce OPN in response to GC B cells via a unique TCR signal.

OPN is expressed locally in GCs of f-BWF1 mice and inhibits BCR-mediated B cell apoptosis

Because diverse cell types can produce OPN, we then examined whether OPN expression was actually enriched in the spontaneous GCs of f-BWF1 mice in situ. Laser-capture microdissection analysis revealed that PNA^+ GC regions in f-BWF1 spleen contained significantly increased *Spp1* transcripts compared with PNA^- regions, indicating de novo OPN activation in GCs; GCs in SRBC-immunized B6 spleen showed no such accumulation of *Spp1* transcripts (Fig. 5A). $CD153^+$ $PD\text{-}1^+$ $CD4^+$ T cells showed a remarkably higher expression of *Spp1* than GC B cells expressing activation-induced cytidine deaminase, and therefore the transcripts were indeed attributable to the $CD153^+$ TF cells (Fig. 5A). Stimulation of the B cells from f-BWF1 mice with anti-μ Ab in vitro resulted in decreased viability, but the effect was significantly rescued in the presence of immobilized OPN, resulting in the enhanced secretion of anti-dsDNA IgG to an extent comparable to anti-CD40 Ab (Fig. 5B). We confirmed that OPN strongly inhibited BCR-induced apoptosis of a B1 cell line, WEHI231 (Fig. 5C). Although anti-μ Ab stimulation alone resulted in the decrease of *Bcl2a1a*, which is crucial for follicular B cell survival (28), OPN significantly enhanced the expression of *Bcl2a1a* (Fig. 5D). The results suggest that OPN produced by $CD153^+$ TF cells in the GCs protects Ag-induced apoptosis of GC B cells.

$CD153^+$ $PD\text{-}1^+$ $CD4^+$ T cells secreting OPN play an essential role in lupus nephritis

Correlating with the increase in SA-T cells with spontaneous GCs, aged B6 mice developed significant anti-histone, anti-dsDNA, and anti-dsDNA IgG Abs in the sera, although the levels tended to be lower than f-BWF1 mice of 5 mo old (Supplemental Fig. 4A). We then finally investigated the involvement of $CD153^+$ $PD\text{-}1^+$ $CD4^+$ T cells in the lupus pathogenesis in f-BWF1 mice. First, to directly examine the role in spontaneous GC reactions, we isolated $PD\text{-}1^-$ $CD4^+$ T cells, $CD153^+$ $PD\text{-}1^+$ $CD4^+$ T cells, and $CD153^-$ $PD\text{-}1^+$ $CD4^+$ T cells from 9-mo-old f-BWF1 mice and transferred them into 6-wk-old f-BWF1 mice, which showed minimal GC development. Because of the limited cell numbers, the purified cells were placed in a temperature-sensitive biogel and injected directly into the spleens. At 3 wk after transfer, the recipients of $CD153^+$ $PD\text{-}1^+$ $CD4^+$ T cells showed a significant increase in GC B cells compared with those of other two populations, and this effect was

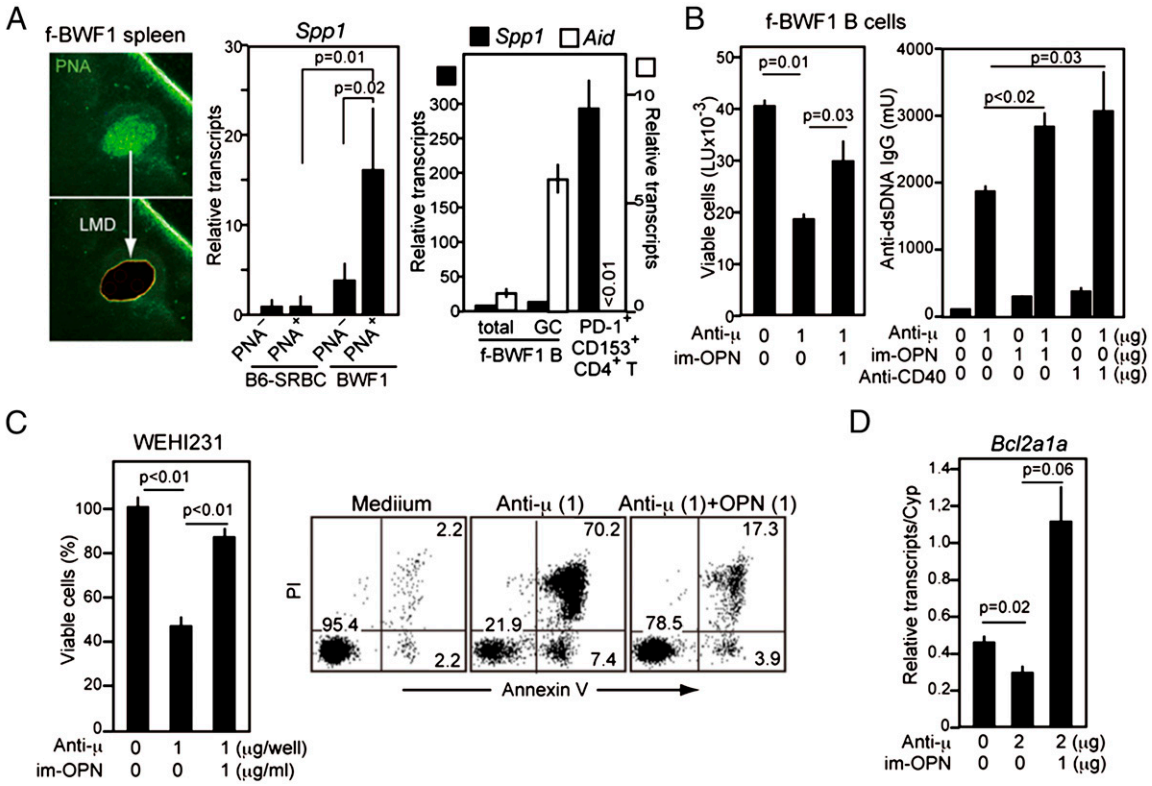

FIGURE 5. *Spp1* transcripts are accumulated in the lupus GCs, and OPN inhibits BCR-mediated B cell apoptosis. (**A**) PNA^+ and PNA^- areas of the spleen sections from 6-mo-old f-BWF1 mice and 3-mo-old B6 mice that were immunized with SRBC 7 d before were laser microdissected, and *Spp1* transcripts were assessed. The means and SEs of three areas are indicated. (**B**) B cells isolated from f-BWF1 mice were cultured in the presence of anti-μ Ab alone or with immobilized (im) OPN or soluble anti-CD40 Ab. Three days later, the viable cells and anti-dsDNA Ab in the culture supernatants were assessed. Means and SEs of triplicate culture are shown. (**C** and **D**) WEHI231 cells were cultured with anti-μ Ab with or without im-OPN. Three days later, the viable cell number was assessed, and aliquots of the cells were analyzed with propidium iodide and anti-annexin V Ab (C). The cells were harvested 4 h after the stimulation, and the transcripts of *Bcl2a1a* were assessed. The means and SEs of triplicate culture are indicated.

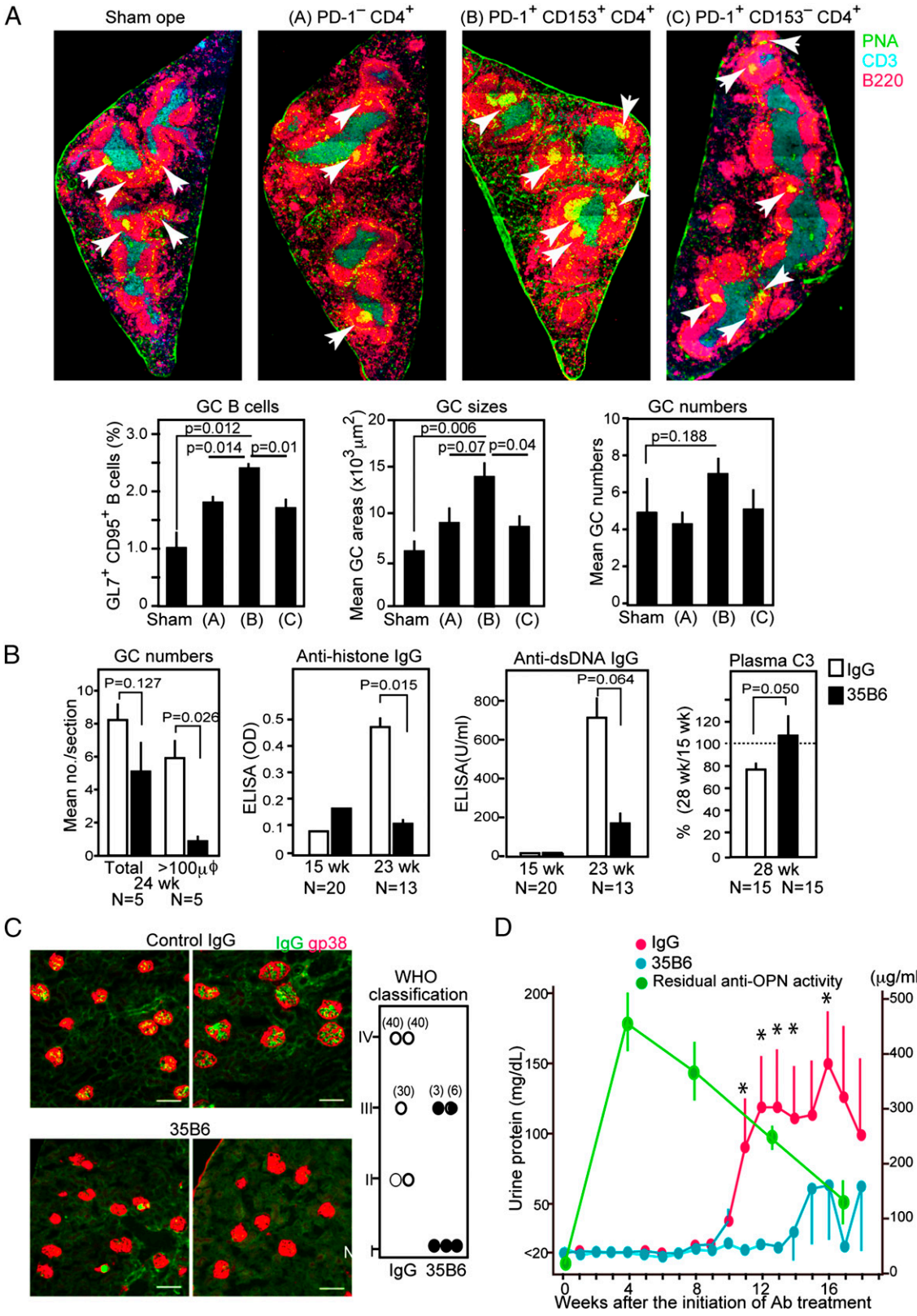

FIGURE 6. CD153+ TF cells play a pathogenic role in lupus disease of f-BWF1 mice. (**A**) PD-1−, PD-1+ CD153+, and PD-1+ CD153−CD4+ T cells were sorted from 9-mo-old f-BWF1 mice and injected into the spleens of 6-wk-old BWF1 mice in temperature-sensitive biogel at 2×10^5 cells per mouse. Three weeks later, the spleens were immunostained with indicated Abs, and the sizes (μm^2) and numbers of GCs (the means of three sections per spleen) were assessed. Representative images of the immunostained spleens are shown. Images of the widest transverse sections are shown at original magnification ×10. Arrowheads indicate PNA+ GCs (*upper*). The numbers of GL-7+ CD95+ GC B cells were analyzed using FACS. The means and SEs of four recipients are shown (*lower*). (**B**–**D**) F-BWF1 mice at the age of 16 wk were administered anti-OPN (35B6) Ab (solid columns) or isotype-matched mouse IgG (open columns) at 500 μg per mouse twice per week. At the age of 24 wk, aliquots of the recipients were sacrificed, and the numbers and sizes of GCs were enumerated in the immunostained tissue sections (two sections per spleen). Means and SEs of five mice are indicated. Anti-dsDNA and anti-histone IgG Abs in the sera were assessed before and after the Ab administration at the indicated ages. Changes in plasma C3 levels after the Ab administration were calculated in individual mice. The means and SEs of the (*Figure legend continues*)

attributable to an increase in individual GC sizes rather than GC numbers (Fig. 6A). Thus, CD153$^+$ PD-1$^+$ CD4$^+$ T cells were capable of enhancing GC expansion in f-BWF1 environment. Although it was unfeasible to follow the fates of transferred cells in vivo due to the small cell numbers, we observed a significant expression of CD153 in a minor fraction of PD-1$^+$ CD153$^-$ cells following anti-CD3 stimulation in vitro (Supplemental Fig. 4B), suggesting that the development of CD153$^+$ T cells from a PD-1$^+$ CD153$^-$ T cell population in vivo might have contributed to the slight increase in GC B cells. We next examined the possible role of OPN. To this end, we administered mouse anti-OPN Ab (35B6) or isotype-matched control mouse IgG to f-BWF1 mice at 500 μg twice per week starting from 16 wk of age. At 24 wk of age, the 35B6-treated mice showed significantly less numbers of large-sized GCs than control mice; concordantly, the development of ANAs was suppressed, with no progression of hypocomplementemia (Fig. 6B). Furthermore, the 35B6-treated mice showed much less glomerular deposition of IgG than control recipients, resulting in ameliorated nephritis scores with minimal glomerular injuries (Fig. 6C). In agreement with the histological findings, the development of proteinuria was also significantly suppressed in 35B6-treated mice at least until plasma anti-OPN activity was attenuated (Fig. 6D). Collectively, these results strongly suggest that CD153$^+$ PD-1$^+$ CD4$^+$ TF cells producing OPN play a crucial role in the development of spontaneous GC reactions and provide an essential, if not sufficient, condition for the development of clinical lupus nephritis in f-BWF1 mice.

Discussion

Cellular senescence is characterized by irreversible arrest of cell proliferation, grossly altered gene expression often associated with a unique signature called SASP, and relative resistance to apoptosis (24). Notably, senescent cells can be metabolically active and may become foci of tissue reactions by secreting various inflammatory factors (29). Although T cell senescence may lead to the reduced capacity of acquired immunity due to the defective Ag-driven clonal proliferation (24), other possible consequences remain to be verified.

An age-dependent PD-1$^+$ CD44^{high}CD4$^+$ T cell population, termed SA-T cells, shows attenuated TCR-induced proliferation, but is capable of secreting abundant OPN (18). Our current results indicated that SA-T cells develop and increase as TF cells in a B cell–dependent manner with age in association with GCs occurring spontaneously, although the cellular features are quite different from those of Ag-driven, regular TFH cells. Robust development of spontaneous GC reactions is a hallmark of lupus disease (8, 9), and we found that the TF cells associated in lupus-prone f-BWF1 mice highly resembled the SA-T cells, except for their much earlier increase, than SA-T cells in B6 mice. First, both SA-T cells in aged B6 mice and TF cells in f-BWF1 mice consisted of two subpopulations defined by the expression of CD153, as follows: CD153$^+$ cell population producing large amounts of OPN and other inflammatory cytokines such as Ccl3 via TCR stimulation with reduced proliferation capacity, and CD153$^-$ cells that were apparently unresponsive to TCR stimulation. Second, both populations showed characteristic signs of cellular senescence, including a remarkable increase in senescence-related genes such as *Ink4b* and *Cip1*, high basal expression levels of several inflammatory genes reminiscent of SASP, a profound decrease of SA-miR-181a, prominent senescence-associated heterochromatic foci in the nuclei, and a high stability in culture. These cell-senescence features were more extensive in CD153$^+$ cells than in CD153$^-$ cells.

The increase of these unique TF cells was correlated with extensive proliferation of CD4$^+$ T cells in vivo, which occurred spontaneously in aged B6 mice and much earlier in f-BWF1 mice. The actively cycling Ki67$^+$ cells were largely confined to PD-1$^+$ CD4$^+$ cell fraction, but CD153$^+$ cells in the PD-1$^+$ CD4$^+$ T cell population barely expressed Ki67 anymore. Considering the characteristic features of cell senescence in the CD153$^+$ PD-1$^+$ CD4$^+$ T cells, it is quite conceivable that the increase of the TF cells is a consequence of extensive CD4$^+$ T cell proliferation in vivo, namely replicative cell senescence. Notably, the senescent CD153$^+$ PD-1$^+$ CD4$^+$ T cells were quite stable in culture, despite the diminished TCR-induced proliferation capacity. The mechanisms underlying such an extensive CD4$^+$ T cell proliferation occurring spontaneously in vivo remain to be verified. A likely mechanism may be homeostatic CD4$^+$ T cell proliferation, which requires tonic TCR signal from self MHC II (30), because the increase of SA-T cells depends on B cells. Age-dependent decline of T cell genesis in normal mice as well as persisted lymphopenia preceding clinical diseases in autoimmune disorders including lupus may endogenously promote the homeostatic CD4$^+$ T cell proliferation (31).

It seems rather paradoxical that CD153$^-$ PD-1$^+$ CD4$^+$ T cells actively cycling in vivo showed no proliferative response to anti-CD3 Ab stimulation at all in vitro with no evidence of activation-induced cell death. Two possibilities may be considered. First, the CD153$^-$ PD-1$^+$ CD4$^+$ cells in ongoing proliferative cell cycles are refractory to an additional potent growth signal via TCR. However, the possibility may not explain the complete TCR unresponsiveness of a whole CD153$^-$ PD-1$^+$ CD4$^+$ T cell population, because all the cells were not in cell cycles at a given time point. Second, these T cells might have been actively imposed of TCR signal unresponsiveness, or TCR anergized, during the proliferation process. Homeostatically proliferating T cells have an intrinsic self-reactivity (32), and our current results indicated that CD153$^+$ PD-1$^+$ CD4$^+$ T cells of f-BWF1 mice specifically responded to autologous B cells dependent on MHC II and TCR in vitro. Potentially self-reactive T cells may fall into a long-standing state of Ag receptor unresponsiveness after encountering specific Ags, termed immunological anergy, which is considered to play a role in peripheral self-tolerance (33, 34). Therefore, a possibility that CD153$^-$ PD-1$^+$ CD4$^+$ T cells are the TCR-anergized cells by the self-tolerance checkpoint is intriguing. If this is the case, CD153$^+$ cells may represent the cells that have escaped from the checkpoint.

The nature of possible self-Ag peptides involved in the activation of CD153$^+$ PD-1$^+$ CD4$^+$ T cells in f-BWF1 mice remains to be elucidated; however, the GC B cells served as the most effective APCs, suggesting that nuclear components captured via BCR and/or TLRs may be involved (35). Curiously, OPN production of CD153$^+$ PD-1$^+$ CD4$^+$ T cells in response to GC B cells was unaffected by PD-1 engagement, although IL-4 production was significantly suppressed. PD-1 signaling is another important checkpoint for potentially self-reactive T cells (36). However, our

indicated numbers of mice are shown (B). At the age of 24 wk, other aliquots of mice (five/each group) were sacrificed, and the kidneys were immunostained with anti-IgG and anti-gp38 Abs. The H&E-stained sections were scored according to the World Health Organization classification. Scale bars, 100 μm. The numbers of injured glomeruli of 40 glomeruli are indicated in the parentheses (C). Urine proteins (red line, control IgG; blue line, 35B6) and the residual activity of 35B6 Ab in the plasma (green line) were assessed once per week and once per month, respectively. *$p < 0.05$.

current results suggest that TCR-induced OPN production of CD153$^+$ TF cells may be mediated via an alternative signaling pathway resistant to PD-1–mediated negative signal, and as such the self-reactive response of CD153$^+$ TF cells may be exempted from PD-1 checkpoint. Notably, the activation of CD153$^+$ TF cells was enhanced by a reverse CD153 signaling via CD30, which is reported to rather inhibit the proliferation and IL-2 production in regular T cells (21, 26). Thus, it seems that CD153 plays a role in a plethora of OPN production by CD153$^+$ TF cells.

Analysis using EGFP-OPN reporter mice suggested that at least a portion of CD153$^+$ SA-T cells in normal aged mice shows spontaneous *Spp1* activation at a given time in vivo. Consistently, *Spp1* transcripts were accumulated in the spontaneous GCs in situ in f-BWF1 mice, conforming to the de novo activation of these TF cells in GCs. OPN is not a typical T cell cytokine; it is expressed in many other cell types, and the range of effects is very broad, including tissue remodeling, inflammation, stress responses, and autoimmunity (37, 38). We indicated that OPN prevents the BCR-induced B cell apoptosis, most likely by inducing the expression of *Bcl2a1a* involved in follicular B cell survival (28). Prolonged survival of the GC B cells, which otherwise have high apoptotic rates, in lupus mice may not only enhance autoantibody production, but accelerate the epitope spreading through somatic hypermutations (14). It is reported that OPN is secreted by myelin-specific pathogenic CD4$^+$ T cells and enhances their survival in experimental autoimmune encephalitis (39). Most recently, it was reported that an intracellular form of OPN plays an important role in sustaining regular TFH cells cell autonomously as an intracellular signal adaptor via Bcl-6 stabilization (40). Although it is possible that an intracellular form of OPN also plays a role in supporting the CD153$^+$ TF cells as a common mechanism for TF cells, the secretion of large amounts of OPN is a unique feature of the CD153$^+$ TF cells, which is barely observed in regular Ag-driven TF cells.

We confirmed the role of CD153$^+$ TF cells in spontaneous GC reactions and lupus pathogenesis. First, we indicated that transfer of the CD153$^+$ PD-1$^+$ CD4$^+$ T cells caused significant increase in GC B cells primarily due to enlarged GCs in young f-BWF1 mice, whereas TCR-unresponsive CD153 PD-1$^+$ CD4$^+$ T cells showed minimal effects. Considering the extremely high proliferation and apoptosis rates of GC B cells, the results may be consistent with their enhanced survival of GC B cells via OPN. We further demonstrated that continuous administration of anti-OPN Ab for 2 mo in f-BWF1 mice significantly suppressed the development of large-sized GCs and ANA production and ameliorated the clinical lupus nephritis. Although it is conceivable that the clinical effect of anti-OPN Ab is primarily attributable to the suppression of spontaneous GC reactions, additional effects on OPN-mediated inflammation in kidney tissues remain possible, because CD153$^+$ PD-1$^+$ CD4$^+$ T cells are also accumulated in the target tissue. In either case, these results strongly suggest that CD153$^+$ PD-1$^+$ CD4$^+$ T cells capable of producing OPN play a crucial, if not sufficient, role in lupus pathogenesis; development of clinical lupus disease in f-BWF1 mice certainly requires other immune cell disorders, including B cells (11). The conclusion is consistent with our previous report that administration of anti–PD-1 Ab, but not anti–PD-L1 Ab, ameliorates the lethal lupus disease in f-BWF1 mice via cell-ablative effect on PD-1$^+$ CD4$^+$ T cells (41). Thus, CD153$^+$ TF cells per se or OPN secreted by them may be a potential therapeutic target for controlling human SLE.

In addition to aging and lupus, we previously reported that SA-T cells also increase rapidly in systemic leukemia, causing an acute reduction of peripheral CD4$^+$ T cell pool (18), and our results indicate that the effect was also associated with robust CD4$^+$ T cell proliferation (Y. Fukushima, Y. Nakashima, and N. Minato, unpublished observations). We propose that an extensive CD4$^+$ T cell proliferation in vivo results in the increase of PD-1$^+$ CD4$^+$ TF cells, with eventual accumulation of senescent CD153$^+$ cells. These senescent TF cells may take a significant part in an increased risk for systemic autoimmunity and inflammation with age and overt autoimmune diseases in specific genetic predispositions. Intervening in their accumulation and/or function may provide novel strategies for controlling human immunosenescence and lupus disease.

Acknowledgments

We thank Drs. N. Yoshikai, K. Iwai, and M. Reth for providing research materials.

Disclosures

The authors have no financial conflicts of interest.

References

1. MacLennan, I. C., and D. Gray. 1986. Antigen-driven selection of virgin and memory B cells. *Immunol. Rev.* 91: 61–85.
2. Zotos, D., and D. M. Tarlinton. 2012. Determining germinal centre B cell fate. *Trends Immunol.* 33: 281–288.
3. Clark, E. A., and J. A. Ledbetter. 1994. How B and T cells talk to each other. *Nature* 367: 425–428.
4. King, C. 2009. New insights into the differentiation and function of T follicular helper cells. *Nat. Rev. Immunol.* 9: 757–766.
5. Nurieva, R. I., Y. Chung, G. J. Martinez, X. O. Yang, S. Tanaka, T. D. Matskevitch, Y. H. Wang, and C. Dong. 2009. Bcl6 mediates the development of T follicular helper cells. *Science* 325: 1001–1005.
6. Yu, D., S. Rao, L. M. Tsai, S. K. Lee, Y. He, E. L. Sutcliffe, M. Srivastava, M. Linterman, L. Zheng, N. Simpson, et al. 2009. The transcriptional repressor Bcl-6 directs T follicular helper cell lineage commitment. *Immunity* 31: 457–468.
7. Ramiscal, R. R., and C. G. Vinuesa. 2013. T-cell subsets in the germinal center. *Immunol. Rev.* 252: 146–155.
8. Grammer, A. C., R. Slota, R. Fischer, H. Gur, H. Girschick, C. Yarboro, G. G. Illei, and P. E. Lipsky. 2003. Abnormal germinal center reactions in systemic lupus erythematosus demonstrated by blockade of CD154-CD40 interactions. *J. Clin. Invest.* 112: 1506–1520.
9. Vinuesa, C. G., I. Sanz, and M. C. Cook. 2009. Dysregulation of germinal centres in autoimmune disease. *Nat. Rev. Immunol.* 9: 845–857.
10. Liu, Z., and A. Davidson. 2012. Taming lupus: a new understanding of pathogenesis is leading to clinical advances. *Nat. Med.* 18: 871–882.
11. Morel, L., B. P. Croker, K. R. Blenman, C. Mohan, G. Huang, G. Gilkeson, and E. K. Wakeland. 2000. Genetic reconstitution of systemic lupus erythematosus immunopathology with polycongenic murine strains. *Proc. Natl. Acad. Sci. USA* 97: 6670–6675.
12. Zouali, M. 2008. B lymphocytes—chief players and therapeutic targets in autoimmune diseases. *Front. Biosci.* 13: 4852–4861.
13. Cappione, A., III, J. H. Anolik, A. Pugh-Bernard, J. Barnard, P. Dutcher, G. Silverman, and I. Sanz. 2005. Germinal center exclusion of autoreactive B cells is defective in human systemic lupus erythematosus. *J. Clin. Invest.* 115: 3205–3216.
14. James, J. A., and J. B. Harley. 1998. B-cell epitope spreading in autoimmunity. *Immunol. Rev.* 164: 185–200.
15. Kim, H. J., B. Verbinnen, X. Tang, L. Lu, and H. Cantor. 2010. Inhibition of follicular T-helper cells by CD8(+) regulatory T cells is essential for self tolerance. *Nature* 467: 328–332.
16. Linterman, M. A., R. J. Rigby, R. K. Wong, D. Yu, R. Brink, J. L. Cannons, P. L. Schwartzberg, M. C. Cook, G. D. Walters, and C. G. Vinuesa. 2009. Follicular helper T cells are required for systemic autoimmunity. *J. Exp. Med.* 206: 561–576.
17. Simpson, N., P. A. Gatenby, A. Wilson, S. Malik, D. A. Fulcher, S. G. Tangye, H. Manku, T. J. Vyse, G. Roncador, G. A. Huttley, et al. 2010. Expansion of circulating T cells resembling follicular helper T cells is a fixed phenotype that identifies a subset of severe systemic lupus erythematosus. *Arthritis Rheum.* 62: 234–244.
18. Shimatani, K., Y. Nakashima, M. Hattori, Y. Hamazaki, and N. Minato. 2009. PD-1+ memory phenotype CD4+ T cells expressing C/EBPalpha underlie T cell immunodepression in senescence and leukemia. *Proc. Natl. Acad. Sci. USA* 106: 15807–15812.
19. Keszei, M., C. Detre, W. Castro, E. Magelky, M. O'Keeffe, K. Kis-Toth, G. C. Tsokos, N. Wang, and C. Terhorst. 2013. Expansion of an osteopontin-expressing T follicular helper cell subset correlates with autoimmunity in B6.Sle1b mice and is suppressed by the H1-isoform of the Slamf6 receptor. *FASEB J.* 27: 3123–3131.
20. Ledermann, B., and K. Bürki. 1991. Establishment of a germ-line competent C57BL/6 embryonic stem cell line. *Exp. Cell Res.* 197: 254–258.

21. Sun, X., H. Yamada, K. Shibata, H. Muta, K. Tani, E. R. Podack, and Y. Yoshikai. 2010. CD30 ligand/CD30 plays a critical role in Th17 differentiation in mice. *J. Immunol.* 185: 2222–2230.
22. Hamamoto, S., T. Yasui, A. Okada, M. Hirose, Y. Matsui, S. Kon, F. Sakai, Y. Kojima, Y. Hayashi, K. Tozawa, et al. 2011. Crucial role of the cryptic epitope SLAYGLR within osteopontin in renal crystal formation of mice. *J. Bone Miner. Res.* 26: 2967–2977.
23. Spolski, R., and W. J. Leonard. 2010. IL-21 and T follicular helper cells. *Int. Immunol.* 22: 7–12.
24. Campisi, J., and F. d'Adda di Fagagna. 2007. Cellular senescence: when bad things happen to good cells. *Nat. Rev. Mol. Cell Biol.* 8: 729–740.
25. Li, G., M. Yu, W. W. Lee, M. Tsang, E. Krishnan, C. M. Weyand, and J. J. Goronzy. 2012. Decline in miR-181a expression with age impairs T cell receptor sensitivity by increasing DUSP6 activity. *Nat. Med.* 18: 1518–1524.
26. Narita, M., S. Nũnez, E. Heard, M. Narita, A. W. Lin, S. A. Hearn, D. L. Spector, G. J. Hannon, and S. W. Lowe. 2003. Rb-mediated heterochromatin formation and silencing of E2F target genes during cellular senescence. *Cell* 113: 703–716.
27. Su, C. C., H. H. Chiu, C. C. Chang, J. C. Chen, and S. M. Hsu. 2004. CD30 is involved in inhibition of T-cell proliferation by Hodgkin's Reed-Sternberg cells. *Cancer Res.* 64: 2148–2152.
28. Ottina, E., F. Grespi, D. Tischner, C. Soratroi, S. Geley, A. Ploner, H. M. Reichardt, A. Villunger, and M. J. Herold. 2012. Targeting antiapoptotic A1/Bfl-1 by in vivo RNAi reveals multiple roles in leukocyte development in mice. *Blood* 119: 6032–6042.
29. Freund, A., A. V. Orjalo, P. Y. Desprez, and J. Campisi. 2010. Inflammatory networks during cellular senescence: causes and consequences. *Trends Mol. Med.* 16: 238–246.
30. Sprent, J., and C. D. Surh. 2011. Normal T cell homeostasis: the conversion of naive cells into memory-phenotype cells. *Nat. Immunol.* 12: 478–484.
31. King, C., A. Ilic, K. Koelsch, and N. Sarvetnick. 2004. Homeostatic expansion of T cells during immune insufficiency generates autoimmunity. *Cell* 117: 265–277.
32. Baccala, R., and A. N. Theofilopoulos. 2005. The new paradigm of T-cell homeostatic proliferation-induced autoimmunity. *Trends Immunol.* 26: 5–8.
33. Schwartz, R. H. 2003. T cell anergy. *Annu. Rev. Immunol.* 21: 305–334.
34. Lohr, J., B. Knoechel, V. Nagabhushanam, and A. K. Abbas. 2005. T-cell tolerance and autoimmunity to systemic and tissue-restricted self-antigens. *Immunol. Rev.* 204: 116–127.
35. Christensen, S. R., and M. J. Shlomchik. 2007. Regulation of lupus-related autoantibody production and clinical disease by Toll-like receptors. *Semin. Immunol.* 19: 11–23.
36. Nishimura, H., M. Nose, H. Hiai, N. Minato, and T. Honjo. 1999. Development of lupus-like autoimmune diseases by disruption of the PD-1 gene encoding an ITIM motif-carrying immunoreceptor. *Immunity* 11: 141–151.
37. Wang, K. X., and D. T. Denhardt. 2008. Osteopontin: role in immune regulation and stress responses. *Cytokine Growth Factor Rev.* 19: 333–345.
38. Lausch, E., A. Janecke, M. Bros, S. Trojandt, Y. Alanay, C. De Laet, C. A. Hübner, P. Meinecke, G. Nishimura, M. Matsuo, et al. 2011. Genetic deficiency of tartrate-resistant acid phosphatase associated with skeletal dysplasia, cerebral calcifications and autoimmunity. *Nat. Genet.* 43: 132–137.
39. Hur, E. M., S. Youssef, M. E. Haws, S. Y. Zhang, R. A. Sobel, and L. Steinman. 2007. Osteopontin-induced relapse and progression of autoimmune brain disease through enhanced survival of activated T cells. *Nat. Immunol.* 8: 74–83.
40. Leavenworth, J. W., B. Verbinnen, J. Yin, H. Huang, and H. Cantor. 2015. A p85α-osteopontin axis couples the receptor ICOS to sustained Bcl-6 expression by follicular helper and regulatory T cells. *Nat. Immunol.* 16: 96–106.
41. Kasagi, S., S. Kawano, T. Okazaki, T. Honjo, A. Morinobu, S. Hatachi, K. Shimatani, Y. Tanaka, N. Minato, and S. Kumagai. 2010. Anti-programmed cell death 1 antibody reduces CD4+PD-1+ T cells and relieves the lupus-like nephritis of NZB/W F1 mice. *J. Immunol.* 184: 2337–2347.